Supporting Information (SI)

Enabling High C$_2$H$_2$ Storage and Efficient C$_2$H$_2$/CO$_2$ Separation in a Cage-like MOF with Multiple Supramolecular Binding Sites

Gang-Ding Wang,[a] Wen-Jie Shi,[b] Yong-Zhi Li,*[c] Weigang Lu,*[a] Lei Hou,*[b] Dan Li[a]

[a]College of Chemistry and Materials Science, Guangdong Provincial Key Laboratory of Supramolecular Coordination Chemistry, Jinan University, Guangzhou 510632, People's Republic of China.

[b]Key Laboratory of Synthetic and Natural Functional Molecule Chemistry of the Ministry of Education, Shaanxi Key Laboratory of Physico-Inorganic Chemistry, College of Chemistry & Materials Science, Northwest University, Xi'an 710069, P. R. China.

[c]School of Materials and Physics, China University of Mining and Technology, Xuzhou 221116, PR China.

*To whom correspondence should be addressed. E-mail: Lyz2021@cumt.edu.cn (Yong-Zhi Li),weiganglu@jnu.edu.cn (Weigang Lu), lhou2009@nwu.edu.cn (Lei Hou).

X-Ray Crystallography

A Bruker Smart Apex II CCD detector was used to collect the single crystal data at 222 K using Mo Kα radiation (λ = 0.71073 Å). The structure was solved by direct methods and refined by full-matrix least-squares refinement based on F^2 with the SHELXTL program. The non-hydrogen atoms were refined anisotropically with the hydrogen atoms added at their geometrically ideal positions and refined isotropically. The SQUEEZE routine of Platon program was applied in refining. The formula of complex was got by the single crystal analysis together with elemental microanalyses and TGA data. Relevant crystallographic results are listed in Table S1. Selected bond lengths and angles are provided in Table S2.

Gas adsorption experiments

Before gas adsorption experiments, the as-synthesized Cu-TPHC samples were immersed in CH_3OH for 72 hours, during which the solvent was decanted and freshly replenished four times a day. Then the samples were activated under vacuum (below 5 μmHg) at 333 K for 4 hours. Gas sorption measurements were then conducted using a Micrometrics ASAP 2020M gas adsorption analyzer.

Breakthrough Experiments

The breakthrough experiment was performed on the Quantachrome dynaSorb BT equipments at 298 and 273 K and 100 kPa with an equal volume of mixed gas (C_2H_2: CO_2: Ar = 5% : 5% : 90% Ar as the carrier gas, flow rate = 5, 10, 15, 20 mL min^{-1}). The activated Cu-TPHC(0.7 g) was filled into a packed column of ϕ 4.2×80 mm, and then the packed column was washed with Ar at a rate of 7 mL min^{-1} at 323 K for 40 minutes to further activate the samples. Between two breakthrough experiments, the adsorbent was regenerated by Ar flow of 5 mL min^{-1} for 35 min at 343 K to guarantee a complete removal of the adsorbed gas.

The C_2H_2 productivity calculations:

The C_2H_2 productivity (q) is defined by the breakthrough amount of C_2H_2, which is calculated by integration of the breakthrough curves f(t) during a period from t1 to t2 where the C_2H_2 purity is higher than or equal to a threshold value:

$$q = \frac{\dfrac{C_i(C_2H_2)}{C_i(C_2H_2) + C_i(CO_2)} \times (\int\limits_{t1}^{t2}\int (t)dt)}{}$$

$$\text{Purity } (C_2H_2) = \frac{signal(C_2H_2)}{signal(C_2H_2) + signal(CO_2)}$$

GCMC Simulation

Grand canonical Monte Carlo (GCMC) simulations were performed for the gas adsorption in the framework by the Sorption module of Material Studio (Accelrys. Materials Studio Getting Started, release 5.0). The framework was considered to be rigid, and the optimized gas and epoxide molecules were used. The partial charges for atoms of the framework were derived from QEq method and QEq neutral 1.0 parameter. One unit cell was used during the simulations. The interaction energies between the gas molecules and framework were computed through the Coulomb and Lennard-Jones 6-12 (LJ) potentials. All parameters for the atoms were modeled with the universal force field (UFF) embedded in the MS modeling package. A cutoff distance of 12.5 Å was used for LJ interactions, and the Coulombic interactions were calculated by using Ewald summation. For each run, the 3×10^6 maximum loading steps, 3×10^6 production steps were employed.

Fitting Adsorption Heat of Pure Component Isotherms

$$\ln P = \ln N + 1/T\sum_{i=0}^{m} a_i N^i + \sum_{i=0}^{n} b_i N^i \qquad Q_{st} = -R\sum_{i=0}^{m} a_i N^i$$

The virial expression was used to fit the combined isotherm data for Cu-TPHC at 273 and 298 K, where P is the pressure, N is the adsorbed amount, T is the temperature, ai and bi are virial coefficients, and m and N are the number of coefficients used to describe the isotherms. Q_{st} is the coverage-dependent enthalpy of adsorption and R is the universal gas constant.

Gas Selectivity Prediction via IAST

The experimental isotherm data for pure gas was fitted using a dual Langmuir-Freundlich (L-F) model:

$$q = \frac{a_1 * b_1 * P^{c1}}{1 + b_1 * P^{c1}} + \frac{a_2 * b_2 * P^{c2}}{1 + b_2 * P^{c2}}$$

Where q and p are adsorbed amounts and the pressure of component i, respectively.

The adsorption selectivities for binary mixtures, defined by

$$S_{i/j} = \frac{x_i * y_j}{x_j * y_i}$$

were respectively calculated using the Ideal Adsorption Solution Theory (IAST). Where x_i is the mole fraction of component i in the adsorbed phase and y_i is the mole fraction of component i in the bulk.

Molecular structure					
Molecular formula	Molecular dimension ($Å^3$)	Kinetic diameter (Å)	Polari $\times 10^{-25}$ (cm^{-3})	Quadrupole moment $\times 10^{-40}$ (Cm^{-2})	Boiling point (K)
C_2H_2	$3.3 \times 3.3 \times 5.7$	3.3	33.3-39.9	+20.5	189.3
CO_2	$3.2 \times 3.3 \times 5.4$	3.3	29.1	-13.4	194.7
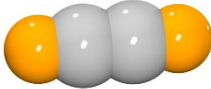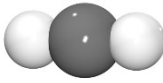
**Scheme S1**. Structures and physical properties of CO_2 and C_2H_2.
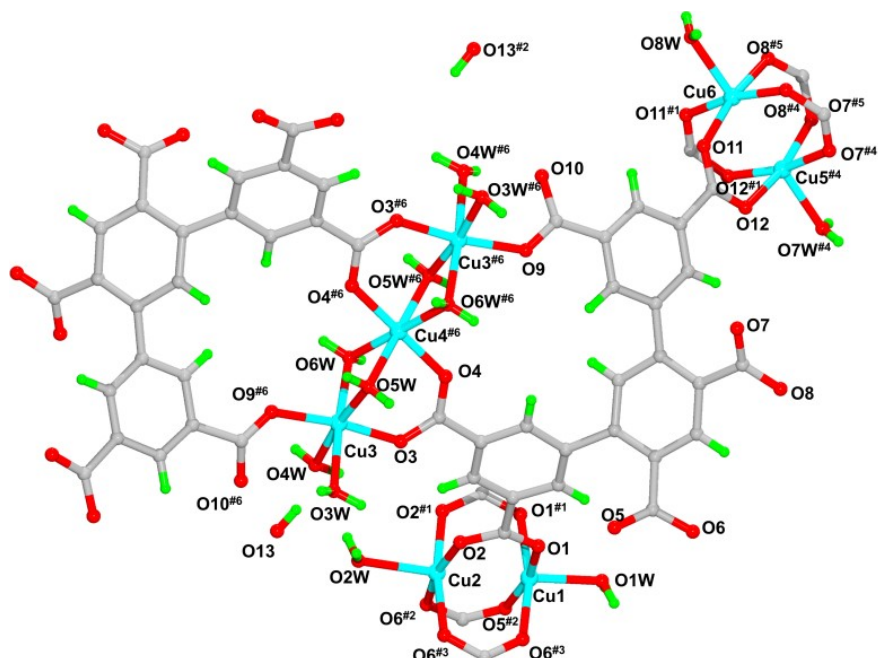
Figure S1. Coordination environment of Cu^{2+} ion in Cu-TPHC.
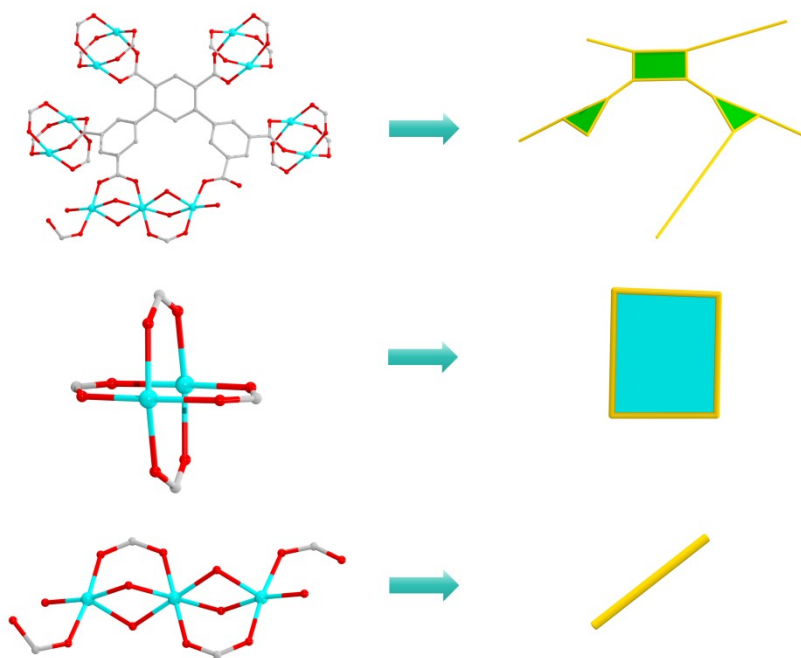
**Figure S2**. Simplification process of TPHC ligands, $[Cu_2(COO)_4]$ paddle-wheel SBU and linear trinuclear $[Cu_3(COO)_2(CO)_2(\mu_2\text{-}OH_2)_4]$ SBU.
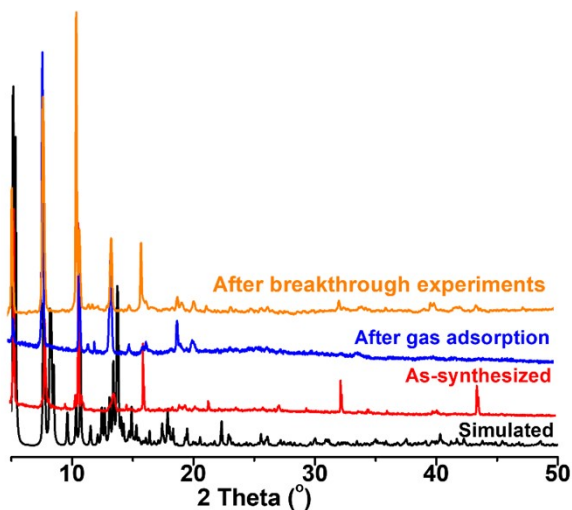

Figure S3. PXRD patterns of simulated, as-synthesized, after gas adsorption and after breakthrough experiments samples of Cu-TPHC.
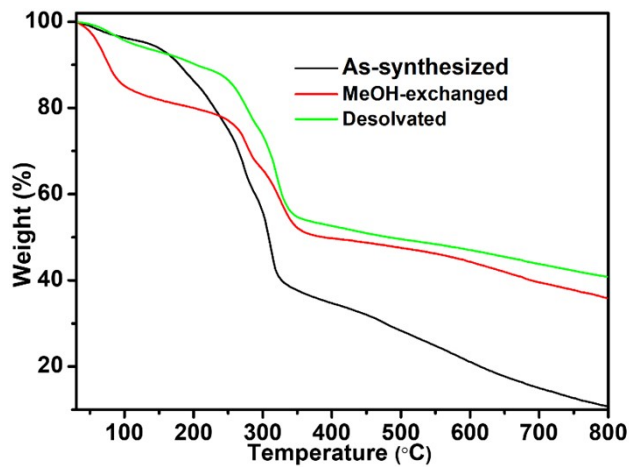
Figure S4. TGA curves of as-synthesized and MeOH-exchanged and desolvated samples of

Cu-TPHC.
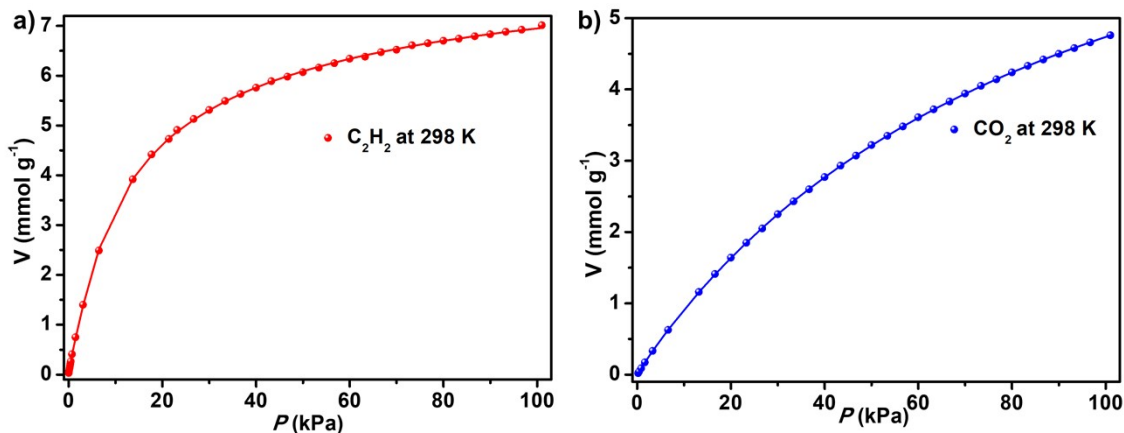
Figure S5. a) C_2H_2 adsorption isotherms of Cu-TPHC with fitted by dual L-F model at 298 K: a1 = 7.16683, b1 = 0.0721, c1 = 0.8417, a2 = 1.3927, b2 = 0.02872, c2 = 1.85497, Chi^2 = 0.00034, R^2 = 0.99996; a) CO_2 adsorption isotherms of Cu-TPHC with fitted by dual L-F model at 298 K: a1 = 8.59892, b1 = 0.00959, c1 = 1.04222, a2 = 0.11331, b2 = 0.23364, c2 = 1.17648, Chi^2 = 0.00001, R^2 = 1.
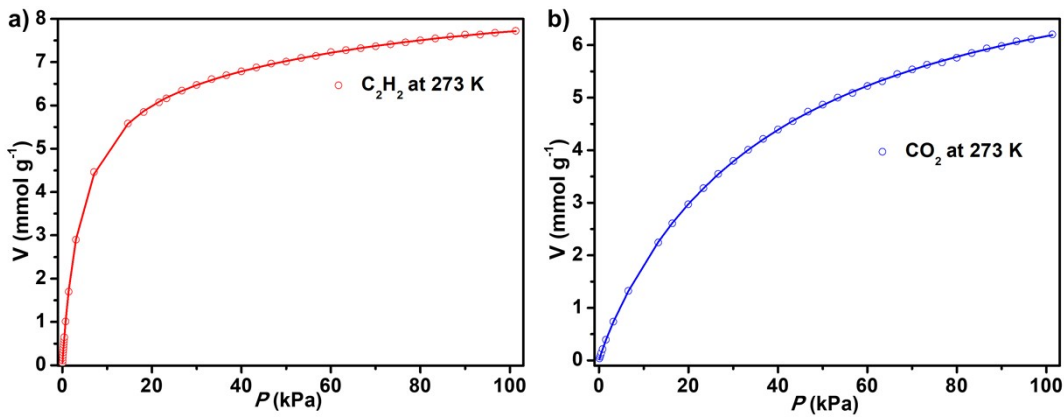
Figure S6. a) C_2H_2 adsorption isotherms of Cu-TPHC with fitted by dual L-F model at 273 K: a1 = 7.35091, b1 = 0.21946, c1 = 0.98209, a2 = 1.09494, b2 = 0.00013, c2 = 2.07672, Chi^2 = 0.00025, R^2 = 0.99998; a) CO_2 adsorption isotherms of Cu-TPHC with fitted by dual L-F model at 273 K: a1 = 8.35652, b1 = 0.0256, c1 = 1.00687, a2 = 0.10939, b2 = 0.91918, c2 = 1.36394, Chi^2 = 0.00014, R^2 = 0.99997.
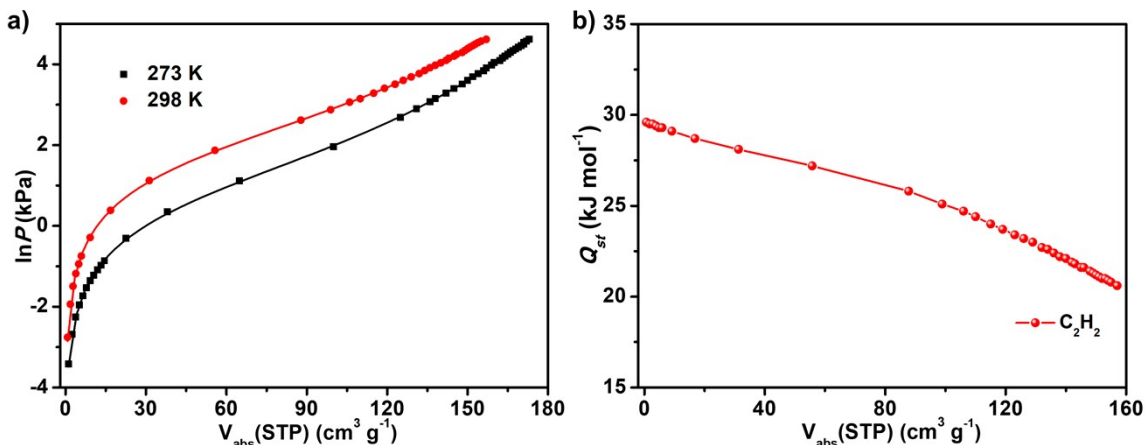
Figure S7. Fitted C_2H_2 isotherms of Cu-TPHC measured at 273 and 298 K, and their corresponding isosteric heats of adsorption (Q_{st}). Fitting results, a0 = -3553.81192, a1 = 5.22566, a2 = -0.00451, a3 = 0.00005, a4 = 2.753E-7, b0 = 9.39269, b1 = -0.01169, b2 = 0.00001, Chi^2 = 0.00049, R^2 = 0.99992.
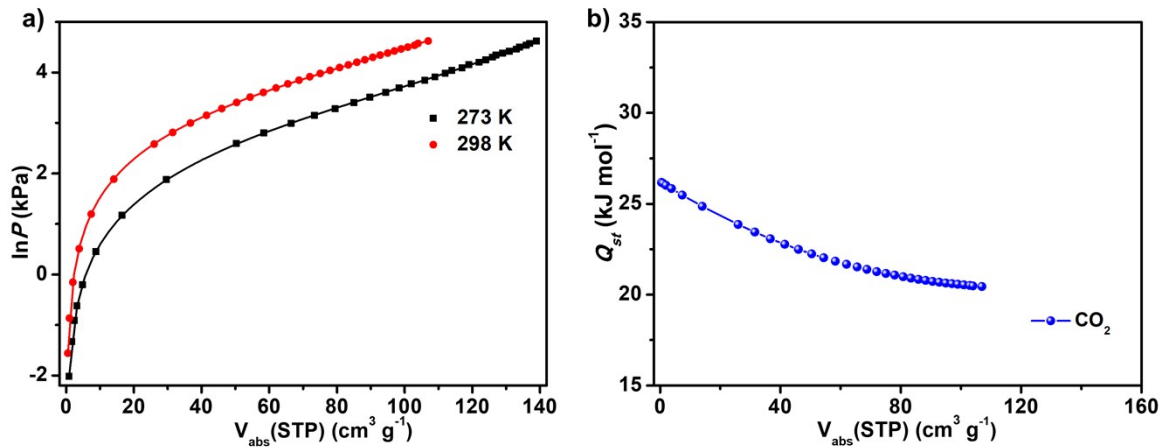
Figure S8. Fitted CO_2 isotherms of Cu-TPHC measured at 273 and 298 K, and their corresponding isosteric heats of adsorption (Q_{st}). Fitting results, a0 = -3154.43651, a1 = 12.6198, a2 = -0.06421, a3 = 0.00003, a4 = 3.2999E-7, b0 = 9.73747, b1 = -0.03508, b2 = 0.00019, Chi^2 = 0.00007, R^2 = 0.99998.
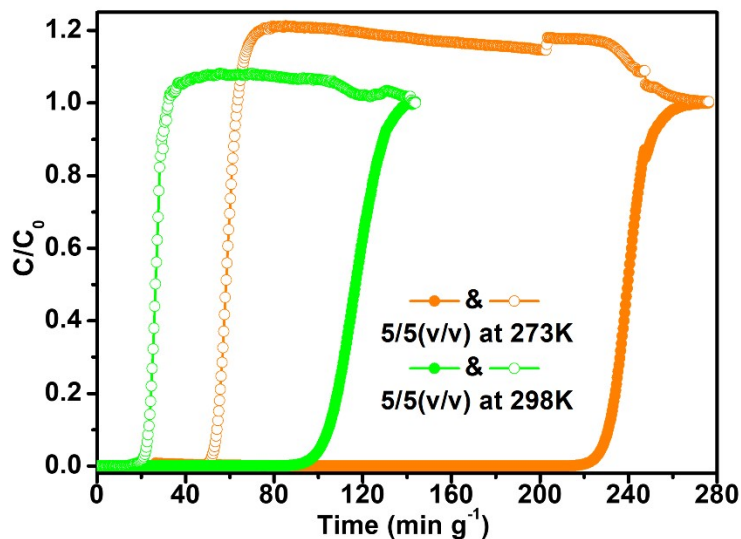
Figure S9. Breakthrough curves for equimolar C_2H_2/CO_2 mixtures at 298 K and 273 K with the flowrate of 5 mL min^{-1}.

Table S1. Crystal Data and Structure Refinements for Cu-TPHC.

Chemical formula	$C_{48}H_{40}Cu_7O_{37}$
Formula weight	1653.58
T (K)	222(2)
Crystal system	Monoclinic
Space group	*P2(1)/m*
a (Å)	18.413(3)

b (Å)	13.933(2)		
c (Å)	22.357(3)		
α(°)	90		
β (°)	111.418(4)		
γ (°)	90		
V (Å^3)	5339.4(13)		
Z	2		
$D_{calcd.}$[g·cm^{-3}]	1.029		
μ (mm^{-1})	1.425		
Goof	1.050		
Reflns	47434/10050/0.0917		
R_1[a], wR_2[b] [I > 2σ]	R_1 = 0.1175, wR_2 =		
R_1[a], wR_2[b] (all data)	R_1 = 0.1336, wR_2 =		

[a]$R_1 = \Sigma(|F_o|-|F_c|)/\Sigma|F_o|$. [b]$R_2 = [\Sigma w(F_o^2 - F_c^2)^2/\Sigma w(F_o^2)^2]^{1/2}$.

Table S2. Selected bond lengths [Å] and angles [°] for Cu-TPHC.

|			
Cu(1)-O(5)#1	1.953(6)	O(6)#2-Cu(2)-O(2W)	97.9(3)
Cu(1)-O(5)#2	1.953(6)	O(2)#3-Cu(2)-O(2W)	93.6(3)
Cu(1)-O(1)#3	1.971(7)	O(2)-Cu(2)-O(2W)	93.6(3)
Cu(1)-O(1)	1.971(7)	O(3)-Cu(3)-O(9)#4	171.2(3)
Cu(1)-O(1W)	2.084(12)	O(3)-Cu(3)-O(6W)	89.1(4)
Cu(2)-O(6)#1	1.945(7)	O(9)#4-Cu(3)-O(6W)	95.4(4)
Cu(2)-O(6)#2	1.945(7)	O(3)-Cu(3)-O(5W)	90.8(4)
Cu(2)-O(2)#3	1.951(7)	O(9)#4-Cu(3)-O(5W)	97.3(4)
Cu(2)-O(2)	1.951(7)	O(6W)-Cu(3)-O(5W)	81.3(5)
Cu(2)-O(2W)	2.292(11)	O(3)-Cu(3)-O(3W)	86.5(6)
Cu(3)-O(3)	1.909(7)	O(9)#4-Cu(3)-O(3W)	89.1(6)
Cu(3)-O(9)#4	1.963(8)	O(6W)-Cu(3)-O(3W)	175.5(6)
Cu(3)-O(6W)	2.047(12)	O(5W)-Cu(3)-O(3W)	97.8(7)
Cu(3)-O(5W)	2.107(12)	O(3)-Cu(3)-O(4W)	83.7(5)
Cu(3)-O(3W)	2.112(16)	O(9)#4-Cu(3)-O(4W)	88.0(5)
Cu(3)-O(4W)	2.14(2)	O(6W)-Cu(3)-O(4W)	102.1(8)
Cu(4)-O(4)#4	1.955(7)	O(5W)-Cu(3)-O(4W)	173.4(7)
Cu(4)-O(4)	1.955(7)	O(3W)-Cu(3)-O(4W)	78.4(9)
Cu(4)-O(5W)	2.108(13)	O(4)#4-Cu(4)-O(4)	180.0000
Cu(4)-O(5W)#4	2.108(13)	O(4)#4-Cu(4)-O(5W)	91.7(3)
Cu(4)-O(6W)#4	2.111(12)	O(4)-Cu(4)-O(5W)	88.3(3)
Cu(4)-O(6W)	2.111(12)	O(4)#4-Cu(4)-O(5W)#4	88.3(3)
Cu(5)-O(12)#5	1.978(7)	O(4)-Cu(4)-O(5W)#4	91.7(3)
Cu(5)-O(12)#6	1.978(7)	O(5W)-Cu(4)-O(5W)#4	180.0000

Cu(5)-O(7)#7	1.982(7)	O(4)#4-Cu(4)-O(6W)#4	89.0(3)
Cu(5)-O(7)	1.982(7)	O(4)-Cu(4)-O(6W)#4	91.0(3)
Cu(5)-O(7W)	2.160(13)	O(5W)-Cu(4)-O(6W)#4	100.2(5)
Cu(6)-O(8)#6	1.958(7)	O(5W)#4-Cu(4)-O(6W)#4	79.8(5)
Cu(6)-O(8)#8	1.958(7)	O(4)#4-Cu(4)-O(6W)	91.0(3)
Cu(6)-O(11)	1.959(8)	O(4)-Cu(4)-O(6W)	89.0(3)
Cu(6)-O(11)#3	1.959(8)	O(5W)-Cu(4)-O(6W)	79.8(5)
Cu(6)-O(8W)	2.203(11)	O(5W)#4-Cu(4)-O(6W)	100.2(5)
O(5)-Cu(1)#2	1.953(6)	O(6W)#4-Cu(4)-O(6W)	180.0000
O(6)-Cu(2)#2	1.945(7)	O(12)#5-Cu(5)-O(12)#6	86.7(4)
O(8)-Cu(6)#6	1.958(7)	O(12)#5-Cu(5)-O(7)#7	92.1(3)
O(9)-Cu(3)#4	1.963(8)	O(12)#6-Cu(5)-O(7)#7	167.4(3)
O(12)-Cu(5)#6	1.978(7)	O(12)#5-Cu(5)-O(7)	167.4(3)
O(5)#1-Cu(1)-O(5)#2	86.9(4)	O(12)#6-Cu(5)-O(7)	92.1(3)
O(5)#1-Cu(1)-O(1)#3	90.8(3)	O(7)#7-Cu(5)-O(7)	86.3(4)
O(5)#2-Cu(1)-O(1)#3	166.6(3)	O(12)#5-Cu(5)-O(7W)	95.8(3)
O(5)#1-Cu(1)-O(1)	166.6(3)	O(12)#6-Cu(5)-O(7W)	95.8(3)
O(5)#2-Cu(1)-O(1)	90.8(3)	O(7)#7-Cu(5)-O(7W)	96.9(3)
O(1)#3-Cu(1)-O(1)	88.5(4)	O(7)-Cu(5)-O(7W)	96.9(3)
O(5)#1-Cu(1)-O(1W)	98.8(3)	O(8)#6-Cu(6)-O(8)#8	88.3(4)
O(5)#2-Cu(1)-O(1W)	98.8(3)	O(8)#6-Cu(6)-O(11)	91.1(3)
O(1)#3-Cu(1)-O(1W)	94.7(3)	O(8)#8-Cu(6)-O(11)	168.3(3)
O(1)-Cu(1)-O(1W)	94.7(3)	O(8)#6-Cu(6)-O(11)#3	168.3(3)
O(6)#1-Cu(2)-O(6)#2	87.2(4)	O(8)#8-Cu(6)-O(11)#3	91.1(3)
O(6)#1-Cu(2)-O(2)#3	91.0(3)	O(11)-Cu(6)-O(11)#3	87.2(5)
O(6)#2-Cu(2)-O(2)#3	168.5(3)	O(8)#6-Cu(6)-O(8W)	95.5(3)
O(6)#1-Cu(2)-O(2)	168.5(3)	O(8)#8-Cu(6)-O(8W)	95.5(3)
O(6)#2-Cu(2)-O(2)	91.0(3)	O(11)-Cu(6)-O(8W)	96.2(3)
O(2)#3-Cu(2)-O(2)	88.4(5)	O(11)#3-Cu(6)-O(8W)	96.2(3)
O(6)#1-Cu(2)-O(2W)	97.9(3)		

Table S3. Comparison of C_2H_2, CO_2 adsorption heats, C_2H_2, CO_2 adsorption uptake, C_2H_2/CO_2 selectivity at 298 K in Cu-TPHC with some top-performing C_2H_2/CO_2 separation materials reported.

Porous materials	C_2H_2 uptake (cm^3 g^{-1})		CO_2 uptake (cm^3 g^{-1})	C_2H_2 Q_{st} (kJ mol^{-1})	CO_2 Q_{st} (kJ mol^{-1})	C_2H_2/CO_2 selectivity	Ref.
	50 kPa	100 kPa					
Cu-TPHC	136.1	157.5	106.1	29.6	26.7	4.9	This work
ZJU-280a	94.9	106.2	71.1	50.6	38.8	18.1	1
JNU-1	53	60	45.5	47.6	--	3.6	2

ZNU-8	71.7	113.1	49.7	27.2	23.4	3.7	3
BUT-155	105	145.1	63.6	30.7	28.1	6.4	4
IPM-101	56	57.1	68.1	43.7	30.7	5.4	5
FJU-6-TATB	69.7	110	58	29	26	3.1	6
NKMOF-1-Ni	55.5	61.0	51.1	60.3	40.9	22	7
ATC-Cu	108	112.2	82.8	79.1	36.5	53.6	8
MOF-OH	55	68.2	26.8	17.5	20.6	25	9
HKUST-1	162	192	137	34.8	26.5	2.4	10
ZJU-50a	167	192	100	40	30.2	12	10
CAU-10-H	77	89.9	60.0	27.5	24.9	4	11
SIFSIX-DPA-Cu-i	64	75.6	50.2	46.5	26.4	9.3	12
$Ni(4\text{-DPDS})_2CrO_4$	65	67	10.1	75.4	37.0	67.7	13
SOFOUR-TEPE-Zn	82	89.1	14.1	45.5	26.3	16833	14
FJU-112	59	74	39	33	23.1	4.2	15
CLCP-1	42	54	37.2	32.7	20.5	3.7	16
FJUT-1	106	133.2	108.4	43.75	37.4	4.06	17
MUF-17	62.9	115.6	93.1	49.5	33.8	6	18
JCM-1	64	75	38	36.9	33	13.7	19
SNNU-27-Ni	106	159	73.5	23.1	16.4	1.9	20

Table S4. Comparison of the C_2H_2/CO_2 breakthrough performance of Cu-TPHC with other materials at 298 K

Porous materials	C_2H_2 uptake (cm^3 g^{-1})	Separation factor	Ref.
Cu-TPHC	157.5	4.4	This work
CAU-10-H	89.9	3.4	11
ZJU-74a	85.7	4.3	21
Cu^I@UiO-66-(COOH)$_2$	51.7	3.4	22
In-L$_6$-IPA	104.4	3.1	23
SNNU-45	134.0	2.9	24
NKMOF-1-Ni	61.0	2.6	7

FJU-6-TATB	110	2.3	6
[Cd(dpip)]	124.4	2.0	25
[Ni(dpip)]	83.6	2.6	26
DNL-9(Fe)	121	2.48	27
HOF-3a	74	2	28
SIFSIX-Cu-TPA	185	1.97	29
FeNi-M'MOF	96	1.7	30

[S1] Q.-L. Qian, X.-W. Gu, J. Pei, H.-M. Wen, H. Wu, W. Zhou, B. Li and G. Qian, A novel anion-pillared metal-organic framework for highly efficient separation of acetylene from ethylene and carbon dioxide, J. Mater. Chem. A, 2021, 9, 9248-9255.

[S2] H. Zeng, M. Xie, Y.-L. Huang, Y. Zhao, X.-J. Xie, J.-P. Bai, M.-Y. Wan, R. Krishna, W. Lu, D. Li, Induced Fit of C_2H_2 in a Flexible MOF Through Cooperative Action of Open Metal Sites, Angew. Chem., Int. Ed., 2019, 58, 8515.

[S3] Y. Zhang, W. Sun, B. Luan, J. Li, D. Luo, Y. Jiang, L. Wang, B. Chen, Topological Design of Unprecedented Metal-Organic Frameworks Featuring Multiple Anion Functionalities and Hierarchical Porosity for Benchmark Acetylene Separation, Angew. Chem. Int. Ed., 2023, 62, e202309925.

[S4] Y.-L. Zhao, Q. Chen, X. Zhang, and J.-R. Li, Enabling C_2H_2/CO_2 Separation Under Humid Conditions with a Methylated Copper MOF, Adv. Sci., 2024, 11, 2310025.

[S5] S. Sharma, S. Mukherjee, A. V. Desai, M. Vandichel, G. K. Dam, A. Jadhav, G. Kociok-Köhn, M. J. Zaworotko, S. K. Ghosh, Efficient Capture of Trace Acetylene by an Ultramicroporous Metal-Organic Framework with Purine Binding Sites, Chem. Mater., 2021, 33, 5800-5808.

[S6] L. Liu, Z. Yao, Y. Ye, Y. Yang, Q. Lin, Z. Zhang, M. O'Keeffe, S. Xiang, Integrating the Pillared-Layer Strategy and Pore-Space Partition Method to Construct Multicomponent MOFs for C_2H_2/CO_2 Separation, J. Am. Chem. Soc., 2020, 142, 9258-9266.

[S7] Y.-L. Peng, T. Pham, P. Li, T. Wang, Y. Chen, K.-J. Chen, K. A. Forrest, B. Space, P. Cheng, M. J. Zaworotko, Z. Zhang, Robust Ultramicroporous Metal-Organic

Frameworks with Benchmark Affinity for Acetylene, Angew. Chem. Int. Ed., 2018, 57, 10971.

[S8] Z. Niu, X. Cui, T. Pham, G. Verma, P. C. Lan, C. Shan, H. Xing, K. A. Forrest, S. Suepaul, B. Space, A. Nafady, A. M. Al-Enizi, S. Ma, A MOF-based Ultra-Strong Acetylene Nano-trap for Highly Efficient C_2H_2/CO_2 Separation, Angew. Chem. Int. Ed., 2021, 60, 5283-5288.

[S9] W. Gong, H. Cui, Y. Xie, Y. Li, X. Tang, Y. Liu, Y. Cui, B. Chen, Efficient C_2H_2/CO_2 Separation in Ultramicroporous Metal-Organic Frameworks with Record C_2H_2 Storage Density, J. Am. Chem. Soc., 2021, 143, 14869-14876.

[S10] K. Shao, H.-M. Wen, C.-C. Liang, X. Xiao, X.-W. Gu, B. Chen, G. Qian, and B. Li, Engineering Supramolecular Binding Sites in a Chemically Stable Metal-Organic Framework for Simultaneous High C_2H_2 Storage and Separation, Angew. Chem. Int. Ed., 2022, 61, e202211523.

[S11] J. Pei, H.-M. Wen, X.-W. Gu, Q.-L. Qian, Y. Yang, Y. Cui, B. Li, B. Chen and G. Qian, Dense Packing of Acetylene in a Stable and Low-Cost Metal-Organic Framework for Efficient C_2H_2/CO_2 Separation, Angew. Chem. Int. Ed., 2021, 60, 25068-25074.

[S12] J. You, H. Wang, T. Xiao, X. Wu, L. Zhang, C.-Z. Lu, Introducing high concentration of hexafluorosilicate anions into an ultra-microporous MOF for highly efficient C_2H_2/CO_2 and C_2H_2/C_2H_4 separation, Chem. Eng. J., 202, 477, 147001.

[S13] F. Zheng, R. Chen, Z. Ding, Y. Liu, Z. Zhang, Q. Yang, Y. Yang, Q. Ren, Z. Bao, Interlayer Symmetry Control in Flexible-Robust Layered Metal-Organic Frameworks for Highly Efficient C_2H_2/CO_2 Separation, J. Am. Chem. Soc., 2023, 145, 19903-19911.

[S14] X. Liu, P. Zhang, H. Xiong, Y. Zhang, K. Wu, J. Liu, R. Krishna, J. Chen, S. Chen, Z. Zeng, S. Deng, J. Wang, Engineering Pore Environments of Sulfate-Pillared Metal-Organic Framework for Efficient C_2H_2/CO_2 Separation with Record Selectivity, Adv. Mater., 2023, 35, 2210415.

[S15] F. Xiang, H. Zhang, Y. Yang, L. Li, Z. Que, L. Chen, Z. Yuan, S. Chen, Z. Yao, J. Fu, S. Xiang, B. Chen, Z. Zhang, Tetranuclear CuII Cluster as the Ten Node Building Unit for the Construction of a Metal-Organic Framework for Efficient C_2H_2/CO_2 Separation, Angew. Chem. Int. Ed., 2023, 62, e202300638.

[S16] Y. Yang, E. Lin, S. Wang, T. Wang, Z. Wang, Z. Zhang, Single-Crystal One-Dimensional Porous Ladder Covalent Polymers, J. Am. Chem. Soc., 2024, 146, 782-790.

[S17] L, Zhang, T. Xiao, X. Zeng, J. You, Z. He, C.-X. Chen, Q. Wang, A. Nafady, A. M. Al-Enizi, S. Ma, Isoreticular Contraction of Cage-like Metal-Organic Frameworks with Optimized Pore Space for Enhanced C_2H_2/CO_2 and C_2H_2/C_2H_4 Separations, J. Am. Chem. Soc., 2024, 146, 7341-7351.

[S18] O. T. Qazvini, R. Babarao, S. G. Telfer, Multipurpose Metal-Organic Framework for the Adsorption of Acetylene: Ethylene Purification and Carbon Dioxide Removal, Chem. Mater., 2019, 31, 4919-4926.

[S19] J. Lee, C. Y. Chuah, J. Kim, Y. Kim, N. Ko, Y. Seo, K. Kim, T. H. Bae, E. Lee, Separation of Acetylene from Carbon Dioxide and Ethylene by a Water-Stable Microporous Metal-Organic Framework with Aligned Imidazolium Groups inside the Channels, Angew. Chem. Int. Ed., 2018, 57, 7869-7873.

[S20] Y.-Y. Xue, X.-Y. Bai, J. Zhang, Y. Wang, S.-N. Li, Y.-C. Jiang, M.-C. Hu, Q.-G. Zhai, Precise Pore Space Partitions Combined with High-Density Hydrogen-Bonding Acceptors within Metal-Organic Frameworks for Highly Efficient Acetylene Storage and Separation, Angew. Chem. Int. Ed., 2021, 60, 10122-10128.

[S21] J. Pei, K. Shao, J.-X. Wang, H.-M. Wen, Y. Yang, Y. Cui, R. Krishna, B. Li, G. Qian, A Chemically Stable Hofmann-Type Metal-Organic Framework with Sandwich-Like Binding Sites for Benchmark Acetylene Capture, Adv. Mater., 2020, 32, 1908275.

[S22] L. Zhang, K. Jiang, L. Yang, L. Li, E. Hu, L. Yang, K. Shao, H. Xing, Y. Cui, Y. Yang, B. Li, B. Chen, G. Qian, Benchmark C_2H_2/CO_2 Separation in an Ultra-Microporous Metal-Organic Framework via Copper(I)-Alkynyl Chemistry, Angew. Chem. Int. Ed., 2021, 60, 15995-16002.

[S23] Y.-Z. Li, G.-Ding Wang, F. Xu, Q. Yin, D. Zhao, J. Qi, Y. Sui, L. Hou, Y.-Yu Wang, A robust indium-organic framework with open tubular channels for efficient separation of acetylene, Nano Res., 2024, 17, 3139-3146.

[S24] Y.-P. Li, Y. Wang, Y.-Y. Xue, H.-P. Li, Q.-G. Zhai, S.-N. Li, Y.-C. Jiang, M.-C. Hu, X. Bu, Ultramicroporous Building Units as a Path to Bi-microporous Metal-Organic Frameworks with High Acetylene Storage and Separation Performance, Angew. Chem.

Int. Ed., 2019, 58, 13590-13595.

[S25]   Y.-Z. Li, R. Krishna, F. Xu, W.-F. Zhang, Y. Sui, L. Hou, Y.-Y. Wang, Z. Zhu, A novel C_2H_2-selective microporous Cd-MOF for C_2H_2/C_2H_4 and C_2H_2/CO_2 separation, Sep. Purif. Technol. 2023, 306, 122678.

[S26]   Y.-Z. Li, G.-D. Wang, L.-N. Ma, L. Hou, Y.-Y. Wang, Z. Zhu, Multiple Functions of Gas Separation and Vapor Adsorption in a New MOF with Open Tubular Channels, ACS Appl. Mater. Interfaces, 2021, 13, 4102-4109.

[S27]   Y.-M. Gu, Y.-Y. Yuan, C.-L. Chen, S.-S. Zhao, T.-J. Sun, Y. Han, X.-W. Liu, Z. Lai and S.-D. Wang, Fluorido-bridged robust metal-organic frameworks for efficient C_2H_2/CO_2 separation under moist conditions, Chem. Sci., 2023,14, 1472-1478.

[S28]   P. Li, Y. He, Y. Zhao, L. Weng, H. Wang, R. Krishna, H. Wu, W. Zhou, M. O'Keeffe, Y. Han, B. Chen, A Rod-Packing Microporous Hydrogen-Bonded Organic Framework for Highly Selective Separation of C_2H_2/CO_2 at Room Temperature, Angew. Chem. Int. Ed., 2015, 54, 574-577.

[S29]   H. Li, C. Liu, C. Chen, Z. Di, D. Yuan, J. Pang, W. Wei, M. Wu, M. Hong, An Unprecedented Pillar-Cage Fluorinated Hybrid Porous Framework with Highly Efficient Acetylene Storage and Separation, Angew. Chem. Int. Ed., 2021, 60, 7547-7552.

[S30]   J. Gao, X. Qian, R.-B. Lin, R. Krishna, H. Wu, W. Zhou, B. Chen, Mixed Metal-Organic Framework with Multiple Binding Sites for Efficient C_2H_2/CO_2 Separation, Angew. Chem. Int. Ed., 2020, 59, 4396-4400.